



# HHS Public Access

Author manuscript

*Annu Rep NMR Spectrosc.* Author manuscript; available in PMC 2019 October 18.

Published in final edited form as:

*Annu Rep NMR Spectrosc.* 2016 ; 89: 103–121. doi:10.1016/bs.arnmr.2016.04.003.

## Orphan spin polarization: A catalyst for high-throughput solid-state NMR spectroscopy of proteins

T. Gopinath<sup>1</sup>, Gianluigi Veglia<sup>1,2,\*</sup>

<sup>1</sup>Department of Biochemistry, Molecular Biology, and Biophysics- University of Minnesota, Minneapolis, MN 55455.

<sup>2</sup>Department of Chemistry– University of Minnesota, Minneapolis, MN 55455.

### Abstract

Magic angle spinning solid-state NMR (MAS ssNMR) spectroscopy is a powerful method for structure determination of biomacromolecules that are recalcitrant to crystallization (membrane proteins and fibrils). Conventional multidimensional ssNMR methods acquire one experiment at a time. This approach is time consuming and discards orphan (unused) spin operators. Relatively low sensitivity and poor resolution of protein samples require long acquisition times for multidimensional ssNMR experiments. Here, we describe our recent progress in the development of multiple acquisition solid-state NMR methods for protein structure determination. A family of experiments called Polarization Optimized Experiments (POE) were designed, in which we utilized the orphan spin operators that are discarded in classical multidimensional NMR experiments, recovering them to allow simultaneous acquisition of multiple 2D and 3D experiments, all while using conventional probes with spectrometers equipped with one receiver. Three strategies namely, DUMAS, MEIOSIS, and MAeSTOSO were used for the concatenation of various 2D and 3D experiments. These methods open up new avenues for reducing the acquisition times of multidimensional experiments for biomolecular ssNMR spectroscopy.

### Keywords

Magic Angle Spinning; Solid-State NMR; SIM-CP; bidirectional SPECIFIC-CP; Residual polarization; Multiple acquisitions; Microcrystalline Proteins; Membrane proteins; DUMAS; MEIOSIS; MAeSTOSO; POE

## (1) Introduction

Magic angle spinning solid-state NMR (MAS ssNMR) spectroscopy is becoming a central technique for chemical, biochemical, and biophysical research, spurring the need for a deeper understanding of theory and its applications to structure, dynamics, and ligand binding of proteins at atomic resolution<sup>1–4</sup>. Higher magnetic field strengths and multidimensional NMR experiments have provided powerful new tools for investigating larger biomacromolecules<sup>5–7</sup>. Unfortunately this comes at the cost of dramatically prolonged

\*To whom correspondence should be addressed: Gianluigi Veglia, Department of Biochemistry, Biophysics, and Molecular Biology, University of Minnesota, 6-155 Jackson Hall, MN 55455. Telephone: (612) 625-0758. Fax: (612) 625-2163. vegli001@umn.edu.

measurement times. In the past few years, several instrumental and methodological developments have increased the scope of ssNMR applications in biomedical research<sup>8–12</sup>. These include the developments of low-E and E-free probes that increase the sensitivity of the RF coil and avoid RF heating caused by high power decoupling pulses<sup>13–15</sup>. The use of dynamic nuclear polarization (DNP) at ultra-low temperatures<sup>16,17</sup>, paramagnetic relaxation enhancement (PRE)<sup>18</sup>, and <sup>1</sup>H detection using ultra-fast MAS probes has dramatically improved the scope of ssNMR for larger biomacromolecules<sup>19,20</sup>. However, all these methods rely on acquiring one experiment at a time leading to longer experimental times.

In spite of tremendous progress in pulse sequence methodology, the ssNMR structure determination is still a time consuming process due to low-throughput multidimensional data acquisition. The conventional ssNMR experiments rely on the detection of single polarization transfer pathway and utilizes only about 5 to 10 % of total experimental time for pulse execution and acquisition of the signal, while 95% time the spectrometer is idle with recycle delay, waiting for completion of longitudinal T<sub>1</sub> relaxation and/or probe duty cycle. To best utilize the NMR polarization we have developed new strategies namely polarization optimized experiments (POE) that concatenates multidimensional experiments by utilizing multiple polarization pathways<sup>21–26</sup>. The first example is DUMAS method that doubles the capability of ssNMR spectrometers via two acquisition periods without repeating the recycle delay. Several pairs of 2D and 3D experiments are concatenated via DUMAS for sequential assignment of proteins<sup>21,22</sup>. DUMAS method is based on simultaneous cross polarization (SIM-CP) that creates two polarization transfer pathways for <sup>13</sup>C and <sup>15</sup>N, which are then used for recording two multidimensional experiments. This is enabled by long T<sub>1</sub> re-laxation of <sup>15</sup>N nuclei which is the fundamental property of all biological solid or semi-solid proteins<sup>27,28</sup>.

The poor sensitivity of conventional ssNMR experiments also results from the incomplete polarization transfer leading to residual spin polarization that is been discarded in conventional experiments. Although it is well known that the existence of residual polarization is a common phenomenon in a cross polarization experiments<sup>29</sup>, it has not been fully exploited in biomolecular ssNMR experiments. In this direction we developed a MEIOSIS and MAeSTOSO methods that utilize the principles of DUMAS, and also uses the residual <sup>13</sup>C and <sup>15</sup>N polarization. Depending on the choice of experiments one can use DUMAS, MEIOSIS, and MAeSTOSO strategies for simultaneous acquisition of multidimensional experiments. We have demonstrated these approaches for simultaneous acquisition of several 2D and 3D experiments thereby representing a universal approach to high-throughput ssNMR spectroscopy of proteins. These methods are applied for structure determination various membrane proteins which are often Challenging to current solid-state NMR methods.

## (2) Overview of single and multiple acquisition MAS solid-state NMR

Recent developments in homonuclear and heteronuclear recoupling schemes enabled efficient polarization transfer thereby facilitating protein sequential assignment of uniformly <sup>13</sup>C and <sup>15</sup>N labeled proteins<sup>26,30–34</sup>. However ssNMR spectroscopy of proteins mainly relies on the detection of heavy atom resonances (<sup>13</sup>C and <sup>15</sup>N) with experiments that are

intrinsically less sensitive than  $^1\text{H}$  detected experiments. Generally, a series of 2D and 3D spectra are necessary to assess the feasibility of structure determination. A schematic of pulse sequence events for conventional (or single acquisition) two-dimensional MAS experiments is shown in Figure 1A. The recycle delay occupies up to 95% of total experimental time while only a fraction of time is used for pulse execution and signal acquisition. Typically, the preparation period consists of  $^1\text{H}$ - $^{13}\text{C}$  or  $^1\text{H}$ - $^{15}\text{N}$  double resonance CP followed by  $t_1$  evolution of  $^{13}\text{C}$  or  $^{15}\text{N}$  coherences. After the  $t_1$  frequency labeling homonuclear and/or heteronuclear mixing periods enable the polarization transfer followed by  $t_2$  acquisition. Similarly a 3D experiment starts with  $^{13}\text{C}$  or  $^{15}\text{N}$  CP followed by multiple evolutions and mixing periods followed by  $^{13}\text{C}$  detection. The main drawback of these single acquisition methods is that a given 2D or 3D pulse sequence can only map any one of the coherence transfer pathways of protein backbone and side chain atoms. For example in a 2D or 3D NCACO and CANCO experiments the polarization pathways for an  $i^{\text{th}}$  residue are given by  $^{15}\text{N}^i \rightarrow ^{13}\text{C}\alpha^i \rightarrow ^{13}\text{CO}^i$ , and  $^{13}\text{C}\alpha^i \rightarrow ^{15}\text{N}^i \rightarrow ^{13}\text{CO}^{i-1}$  respectively, and this requires two separate experiments.

Inspired by the previous work of Pines and Waugh<sup>29</sup>, we asked ourselves: how to create multiple polarization pathways and detect them in a single experiment?. In fact, Waugh and coworkers have utilized the rich  $^1\text{H}$  bath for multiple  $^{13}\text{C}$  CP acquisitions while holding the proton polarization in the transverse plane under continuous wave decoupling. Although the application of this method on current biological systems is limited due to shorter relaxation ( $T_{1\rho}$  and  $T_2$ ) times, it however demonstrated the source of hidden polarization in the  $^1\text{H}$  spin bath of solid samples. Another unique property in ssNMR is the long  $T_1$  relaxation of low-abundant nuclei, in particular  $^{15}\text{N}$  nuclei of solid proteins can have few hundred milliseconds of  $T_1$  relaxation<sup>28</sup>. Based on these two unique features of solid systems we have pioneered Multiple acquisition solid-state NMR of proteins that follows the philosophy of multiple  $^{13}\text{C}$  acquisitions using single receiver while simultaneously storing the other spin operators in the form of  $^{15}\text{N}$  longitudinal polarization that will then be transferred to  $^{13}\text{C}$  and detected in the following acquisitions. A schematic of multiple acquisition MAS ssNMR is shown in Figure 1B, where a single recycle delay is used for acquiring two to eight experiments resulting from different polarization pathways. The novel feature of multiple acquisition schemes is that it not only records the conventional or parent experiment in the first acquisition but also stores the orphan (unused) spin polarization which will then be used in the subsequent acquisitions.

To this end we have designed three different strategies namely, DUMAS, MEIOSIS, and MAeSTOSO for concatenation of multi-dimensional experiments into a single pulse sequence<sup>21-23,25</sup>. For example a 2D or 3D DUMAS-NCACO-CANCO experiment acquires  $^{15}\text{N}^i \rightarrow ^{13}\text{C}\alpha^i \rightarrow ^{13}\text{CO}^i$ , and  $^{13}\text{C}\alpha^i \rightarrow ^{15}\text{N}^i \rightarrow ^{13}\text{CO}^{i-1}$  polarization pathways in a single experiment. Figure 2A shows the various two and three-dimensional experiments that are respectively represented in rectangles and cubes. Few examples of concatenation of two and three dimensional experiments using DUMAS, MEIOSIS, and MAeSTOSO are shown in Figure 2B. While DUMAS approach records two spectra from dual polarization pathways (section 3), MEIOSIS and MAeSTOSO can record four to eight multi-dimensional spectra using transferred and residual polarization pathways (sections 4 and 5).

### (3) Creation of dual polarization pathways and simultaneous acquisition of multidimensional experiments

In ssNMR, the evolution of spin operators is dictated by dipolar couplings. Unlike in liquid-state NMR, the  $^{13}\text{C}$  and  $^{15}\text{N}$  edited experiments start with a single spin operator of  $^{13}\text{C}$  or  $^{15}\text{N}$  magnetization generated from the abundant spin ( $^1\text{H}$ ) via Hartmann-Hahn (HH) cross-polarization. The CP transfer efficiency is affected by the overall dipolar coupling network of homo- and heteronuclear spins of the system under consideration<sup>32,35</sup>. Figure 3A shows  $^{13}\text{C}$  and  $^{15}\text{N}$  edited CXCX and NCA correlation experiments and evolution of corresponding spin operators during the course of the pulse sequence. In both cases, the preparation period uses a double resonance CP to create initial  $^{13}\text{C}$  or  $^{15}\text{N}$  polarization followed by  $t_1$  chemical shift evolution, mixing and  $^{13}\text{C}$  detection during  $t_2$  period. CXCX and NC correlations are respectively obtained from homo and hetero nuclear mixing periods such as DARR and Specific-CP<sup>30,31</sup>.

The rich proton spin bath can be used to create two polarization pathways ( $^{13}\text{C}$  and  $^{15}\text{N}$ ) using simultaneous cross polarization (SIM-CP). In this this approach (Figure 3B), namely DUMAS, SIM-CP represents the preparation period that creates initial  $^{13}\text{C}$  and  $^{15}\text{N}$  polarization which will then be used for acquiring  $^{13}\text{C}$  and  $^{15}\text{N}$  edited experiments in first and second acquisitions respectively. Figure 3B shows pulse sequence for simultaneous acquisition of CXCX and NCA experiments, dual polarization pathways at various stages of pulse sequence are also shown. During SIM-CP the RF amplitudes of both the  $^{13}\text{C}$  and  $^{15}\text{N}$  channels simultaneously satisfy the Hartmann-Hahn matching condition with respect to  $^1\text{H}$  RF amplitude and MAS rate. It was found that the sensitivity of CP and SIM-CP are similar for  $^{13}\text{C}$ , whereas only a marginal loss (less than 10 %) of sensitivity was observed for  $^{15}\text{N}$  using SIM-CP<sup>24</sup>. It is to be noted that the SIM-CP performance is benefited from strong  $^1\text{H}$ - $^1\text{H}$  dipolar coupling network that enables efficient spin diffusion thereby providing almost similar sensitivity for  $^{13}\text{C}$  and  $^{15}\text{N}$  with respect to double resonance CP. Following SIM-CP, CXCX experiment is acquired in the first acquisition while storing the  $^{15}\text{N}$  polarization along z-direction. The  $^{15}\text{N}$  polarization is then utilized for acquiring NC correlation experiment during second acquisition.

Successful application of DUMAS requires a rough estimation of relative sensitivity of independent experiments. For example,  $^{13}\text{C}$ - $^{13}\text{C}$  polarization transfer under PDSO or DARR is affected by several factors including short and long range dipolar couplings, orientation and scaling of anisotropic interactions of a given protein sample, and rate of magic angle spinning. Thus a given DARR mixing time provides  $^{13}\text{C}$ - $^{13}\text{C}$  transfer for broad range of distances. To achieve reasonable sensitivity for intra-residue backbone and side chain correlations it is often necessary to use multiple short mixing times ranging from 10 to 40 ms. Aromatic intra-residue correlations can sometimes require up to 100 ms mixing time due to extensive dynamics. On the other hand medium and long range inter-residue or inter protomer correlations are obtained from longer mixing times of 100 to 500 ms. Similarly one may have to use multiple DARR mixing times for NCACX and NCOCX 2D correlation experiments. However longer DARR mixing times dramatically reduce the sensitivity of the experiments due to multiple correlations as well as  $T_1$  relaxation.

The 2D DUMAS experimental scheme is well suited for optimizing the sensitivity for multiple DARR mixing times for  $^{13}\text{C}$  and  $^{15}\text{N}$  edited experiments. A novel aspect of DUMAS experiments is that the  $^{13}\text{C}$  evolution followed by mixing period does not affect the  $^{15}\text{N}$  polarization which is stored along z-direction (Figure 3). Therefore, multiple CXCX experiments with different mixing times can be obtained during first acquisition without disturbing the second acquisition NC experimental parameters, and vice versa. Figure 4 shows two examples of 2D DUMAS experiments on ubiquitin and sarcolipin membrane protein. In Figure 4A both CXCX-20ms and CXCX-100ms experiments were acquired during the first acquisition with an experimental time of 12 and 24 hours respectively, while the NCACX in the second acquisition utilizes all 36 hours of signal averaging. From technical point of view this is done by creating two data acquisition files, where the CXCX mixing was set to 20 and 100 ms in first and second files respectively and second acquisition parameters are identical in both the files. After the completion of two experiments the CXCX data is processed separately whereas the second acquisition NCACX data was added from two files. Similarly one can also switch the second acquisition experiments without effecting the first acquisition, as shown in Figure 4B for sarcolipin membrane protein. In this case CXCX-20 ms experiment was acquired in the first acquisition, whereas second acquisition acquires both NCA and NCO. The DUMAS approach can be used for the concatenation of several pairs two and three dimensional experiments. An example of 3D DUMAS experiment for simultaneous acquisition of NCACX and CANCO is shown in Figure 5.

#### **(4) Deconvolution of transferred and residual polarization pathways enables the acquisition of multiple two and three-dimensional experiments**

In the quest of multiple polarization pathways, we examined the cross polarization density matrix operators. In fact, during the CP between two spin baths I and S (I, S =  $^1\text{H}$ ,  $^{13}\text{C}$ ,  $^{15}\text{N}$ ), there is always a residual magnetization that remains on I spin<sup>35</sup>. This phenomenon can be understood by the characterization the CP dynamics in DQ (double quantum) and ZQ (zero quantum) sub-spaces. In fact only a part of I-spin polarization, namely ZQ operator, is perpendicular to ZQ dipolar Hamiltonian and evolves during CP, the combination of  $^1\text{H}$ - $^1\text{H}$  spin diffusion and  $T_{1\rho}$  relaxation leads to incomplete polarization transfer. In the conventional methods the residual magnetization is often cancelled out by a z-filter or phase cycling to suppress the artifacts that may interfere with the desired polarization pathway of interest. Here we focus on recovering the residual polarization pathways of NC and CN selective cross polarization obtained from Specific-CP which is basic building block of almost all triple resonance ssNMR experiments. In particular, we demonstrate that in a single pulse sequence, the combination of SIM-CP and Specific-CP creates four polarization pathways that can be used for recording four different experiments utilizing two acquisitions per scan. This method, called MEIOSIS (Multiple Experiments via Orphan Spin operatorS), can be used for both 2D and 3D experiments<sup>23</sup>.

Figure 6A shows an example of 2D MEIOSIS pulse sequence, the spin operators of  $^1\text{H}$ ,  $^{13}\text{C}$  and  $^{15}\text{N}$  nuclei at various steps of the pulse sequence are shown in Figure 6B. The pulse sequence starts with simultaneous cross polarization of  $^{13}\text{C}$  and  $^{15}\text{N}$  followed by parallel

evolutions represented by  $t_1'$  and  $t_1''$  respectively. An NCA/CAN specific-CP is then used to create four magnetization pathways: NCA, NN, CAN, and CC. The NCA and CAN refers to polarization transferred from N to C $\alpha$  and vice versa, while NN and CC result from the residual magnetization remaining on  $^{15}\text{N}$  and  $^{13}\text{C}$  nuclei that is not transferred to  $^{13}\text{C}$  and  $^{15}\text{N}$  during NCA specific-CP. A DARR mixing period sandwiched between two  $90^\circ$  pulses is applied to NCA and CC pathways followed by  $t_2'$  acquisition, while the magnetization arising from the other two pathways (CAN and NN) is stored as  $^{15}\text{N}$  z-magnetization. After the first acquisition, the  $^{15}\text{N}$  magnetization is transferred to the  $^{13}\text{CO}$  group followed by a second FID, which gives the  $^{13}\text{C}$  spectrum resulting from the CAN and NN pathways. The first acquisition gives sum of two 2D spectra CXCX and NCACX resulting from CC and NCA pathways respectively. While the second FID is the sum of NCO and CA(N)CO 2D spectra resulting from NN and CAN pathways respectively. In order to decode the two pathways in each acquisition, we alternate the phase of the specificCP  $^{15}\text{N}$  spin-lock between +x and -x. The resultant spectra for +x and -x phases are stored in separate memory allocations. Since the NCA and CAN transfer occur in a doubly tilted rotating frame, the phase switching of  $^{15}\text{N}$  spin-lock during specific-CP will invert the sign of the NCA and CAN transfer, whereas the residual CC and NN magnetization will not be effected by the phase alternation. Thus the addition and subtraction of two data sets with phases +x and -x respectively gives DARR and NCACX in first acquisition, and NCO and CANCO in the second acquisition.

Figure 6C shows the amplitudes of four pathways as a function of NCA/CAN specific-CP contact time. The maximum of the NCA (or CAN) transfer occurs at approximately at 3 ms contact time, whereas the residual magnetization corresponds to, ~35 % for  $^{15}\text{N}$ , ~43% for the  $^{13}\text{CO}$ , and ~52%  $^{13}\text{C}$  aliphatic resonances. Figure 6D shows application of MEIOSIS approach for simultaneous acquisition of CXCX, NCACX, CANCO, and NCO experiments on U- $^{13}\text{C}$ - $^{15}\text{N}$  ubiquitin sample. Remarkably, the total experimental time for four experiments acquired simultaneously with the MEIOSIS sequence was ~29 hours, whereas the total experimental time for conventional single acquisition experiments was ~62hours, with CXCX and NCACX experiments acquired in 7 and 22 hrs, respectively, and NCO and CA(N)CO experiments took 3.5 and 28 hours, respectively. Similarly other combinations of CC, NCC, CNC, and NC correlation experiments can be concatenated using MEIOSIS approach<sup>24</sup>.

The MEIOSIS approach is another example of polarization optimized experiments (POE) that recover the residual magnetization to speed-up the data acquisition. The two-dimensional MEIOSIS experiments can be used to assess the resolution and sensitivity of the spectra and make an educated decision on which dimension of the multidimensional spectra need to be acquired with higher resolution for more efficient resonance assignment. The MEIOSIS method can also extended to 3D experiments by incorporating an additional  $^{13}\text{C}$  evolution period prior to the first and second acquisitions. For example, three 3D experiments NCACX, NCOCX and CA(N)COCX were obtained from NCA, NN, and CAN pathways, respectively<sup>23</sup>.

## (5) How far can we push the residual polarization?

The current progress in biological solid-state NMR is greatly benefited from the advancements in NMR hardware including the developments of low-E or E-free probes that avoid RF heating caused by high power decoupling pulses. In fact these technological developments were crucial for successful implementation of DUMAS and MEIOSIS dual acquisition experiments. Here, in order to fully utilize the residual polarization, we incorporate four acquisitions, namely MAeSTOSO approach that is a direct extension of 2D DUMAS and MEIOSIS. MAeSTOSO-4 and MAeSTOSO-8 simultaneously acquires four and eight two-dimensional experiments respectively utilizing four acquisition per scan<sup>25</sup>. The first two acquisitions of MAeSTOSO-4 and MAeSTOSO-8 resembles DUMAS and MEIOSIS respectively. The main idea behind MAeSTOSO experiments is to use the residual polarization resulting from multiple NC periods, for acquiring additional experiments by incorporating two more acquisitions. In a single experiment MAeSTOSO-4 acquires a CC and NC experiments in the first and second acquisitions, and two more NC experiments are recorded in third and fourth acquisitions by utilizing ~30% and ~10% residual polarization respectively. Similarly, MEIOSIS can be extended to MAeSTOSO-8 to record eight experiments using four acquisitions per scan.

An example of MAeSTOSO-8 on U-<sup>13</sup>C-<sup>15</sup>N ubiquitin is shown in figure 7 for simultaneous acquisition of eight experiments, CXCX and NCACX in the first acquisition, a pair of CA(N)COCX and NCOCX with CC mixing times of 20 and 40 ms acquired in second and third acquisitions respectively, and the fourth acquisition records CA(N)CO and NCO. The two pathways in each acquisition were deconvoluted by addition and subtraction of two data sets obtained by switching the phase of <sup>15</sup>N spin lock of NCA period. Schematic of polarization pathways at various stages of pulse sequence is shown in figure 7B. Because of polarization sharing at each NC step, the magnitude of residual polarization decreases with number of NC periods, leading to only 1% of polarization available for the fourth acquisition. Out of eight experiments NCACX-200ms and CA(N)CACX-40ms utilize the initial polarization from SIM-CP, and hence the sensitivity is similar to conventional experiments that are acquired via single acquisition methods. Whereas the remaining six experiments utilize either <sup>13</sup>C or <sup>15</sup>N residual polarization resulting in a lower sensitivity with respect to corresponding 2D experiments acquired separately using same number of scans. Using same number of  $t_1$  increments as of 2D MAeSTOSO-8, conventional single acquisition 2D NCOCX and CO(N)CACX 2D spectra will require 10 days each, whereas CXCX, NCACB, CO(N)CACB, NCACX, CO(N)CACX, CO(N)CA, and NCA will need 5, 5, 5, 6, 6, and 1 days respectively. In total, the eight 2D experiments will require about 25 days if acquired separately using conventional methods in comparison to 10 days of total experimental time using MAeSTOSO-8, demonstrating a time saving of 70%. Similarly, MAeSTOSO can be used for other combinations of CC, CNCC, NCC experiments. To optimize the sensitivity of MAeSTOSO experiments one should acquire insensitive experiments in first two acquisitions that require larger number of scans thereby accumulating sufficient residual polarization to drive third and fourth acquisitions. As shown in figure 7C, the spectra acquired in first two acquisitions require more number of scans due

to longer DARR mixing periods; this enables sufficient residual polarization for third and fourth acquisitions.

## (6) Choosing DUMAS, MEIOSIS and MAeSTOSO strategies for simultaneous acquisition of ssNMR experiments

The inefficiency of the polarization transfer schemes together with undetected (orphan) spin operators contribute to the intrinsic insensitivity of the ssNMR experiments. DUMAS, MEIOSIS, and MAeSTOSOS represent a class of polarization optimized experiments (POE) that optimize the sensitivity by recovering the orphan spin operators to obtain multiple NMR experiments. A key feature of these experiments is that the amplitudes of these spin operators are different for each path way. Therefore, depending on the sensitivity of the experiments, one can chose one of these strategies for multiple data acquisitions. In general, protein sequential assignment begins with the acquisition of 2D CXCX, NC, CNC and NCC correlation experiments using shorter CC mixing times of 10 to 30 ms. These experiments can be simultaneously acquired by 2D DUMAS and MEIOSIS. Note that MEIOSIS can be used only if one of the experiments is CNC or CNCC. The finger prints obtained from these 2D spectra demonstrate the quality of spectral resolution as well as the sensitivity of a given protein sample. Robust backbone assignment can then be obtained by 3D-DUMAS-NCACX-CANCO or 3D-MEIOSIS NCACX-NCOCX-CA(N)COCX. Depending on the complexity of spectral overlap one may have to repeat these experiments with multiple mixing times, as we as the use of residue specific isotope labeling schemes. Recent studies on membrane proteins have shown that the spectral resolution can be improved by using water-edited experiments as well as the use of reverse unlabeled of hydrophobic residues<sup>36,37</sup>. In fact these methodologies can be further improved by using multiple acquisition methods.

While DUMAS and MEIOSIS strategies are preferable for shorter CC mixing times, MAeSTOSO is more suitable for acquiring low sensitivity experiments, e.g., 2D CXCX (100–200 ms mixing time) or NCOCX (100–200 ms mixing times) that require a significantly higher number of scans. In this case the MAeSTOSO strategy is preferable as the accumulation of residual polarization is such that one can acquire simultaneously a greater number of experiments and optimize the total experimental time. Typically, longer mixing times are necessary to obtain long range distance restraints for protein structure determination<sup>38–40</sup>. These experiments require several days of signal averaging for insensitive samples such as those of membrane proteins. One may also use selective or differential labeling schemes for obtaining unambiguous long-range correlations<sup>39</sup>. In this case the bonus experiments obtained from MAeSTOSO can be compared with other data for cross checking the assignment. Thus MAeSTOSO can represent a cost-effective solution to acquire multiple experiments.

## (7) Conclusions and outlook

The polarization optimized experiments (POE) presented in this chapter will bring a new dimension in ssNMR methodology by integrating various NMR pulse sequences using state-of-art NMR probe technology. More importantly this approach doesn't overwrite the



existing experiments, but rather provides a clever strategy to concatenate multiple experiments into a single pulse sequence. Using classical setup of ssNMR spectrometers multiple 2D and 3D experiments can be acquired, reducing by half the experimental time. The overall philosophy of the POE approach is to make the best out of the polarization generated. In fact the existence of unused polarization (orphan spin operators) was first pointed out by Pines et al. in the implementation of  $^1\text{H}$  enhanced experiments via multiple cross polarization acquisitions<sup>29</sup>. Historically, the solution NMR community has been the most attentive to detect multiple spin operators for simultaneous acquisition of 2D experiments such as COSY–NOESY and COCONOSY and/or enhance the signal<sup>41</sup>. Takegoshi and co-workers have implemented the equivalent of COCONOSY for solids as well as the double acquisition using discarded coherences in 2D spectra with the States method<sup>42,43</sup>, paving the way for multiple acquisitions in biological solids. More recently, the afterglow phenomenon exploited by Kay and co-workers opened up the possibility for the acquisition of multidimensional NMR spectra of proteins in parallel<sup>44,45</sup>. The latter approach has been implemented with either one or multiple receivers. While all these methods combine only a specific type of experiments, the POE experiments presented here represent a universal approach for multiple acquisitions of almost all types of double and triple resonance  $^{13}\text{C}$  detected experiments. Finally, when applied in concert with other fast acquisition and sensitivity enhancement techniques (e.g., Dynamic Nuclear Polarization, Paramagnetic Relaxation Enhancements, etc.) this approach can further push the boundaries of ssNMR applications to structural biology.

## Acknowledgements

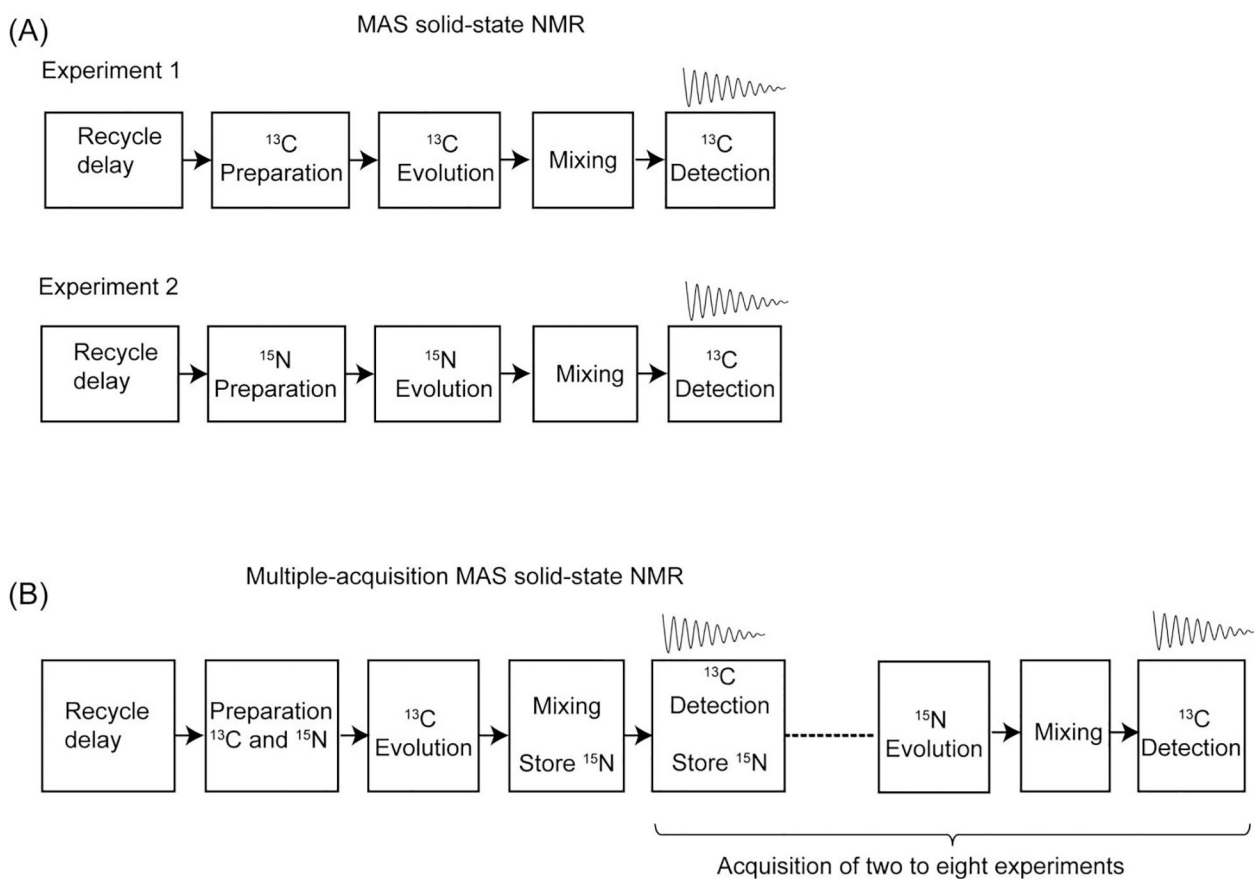
The experiments were carried out at Minnesota NMR Center with the support of National Institute of Health (GM64742). We thank current and former members of Veglia group for helpful discussions and preparing NMR samples.

## References

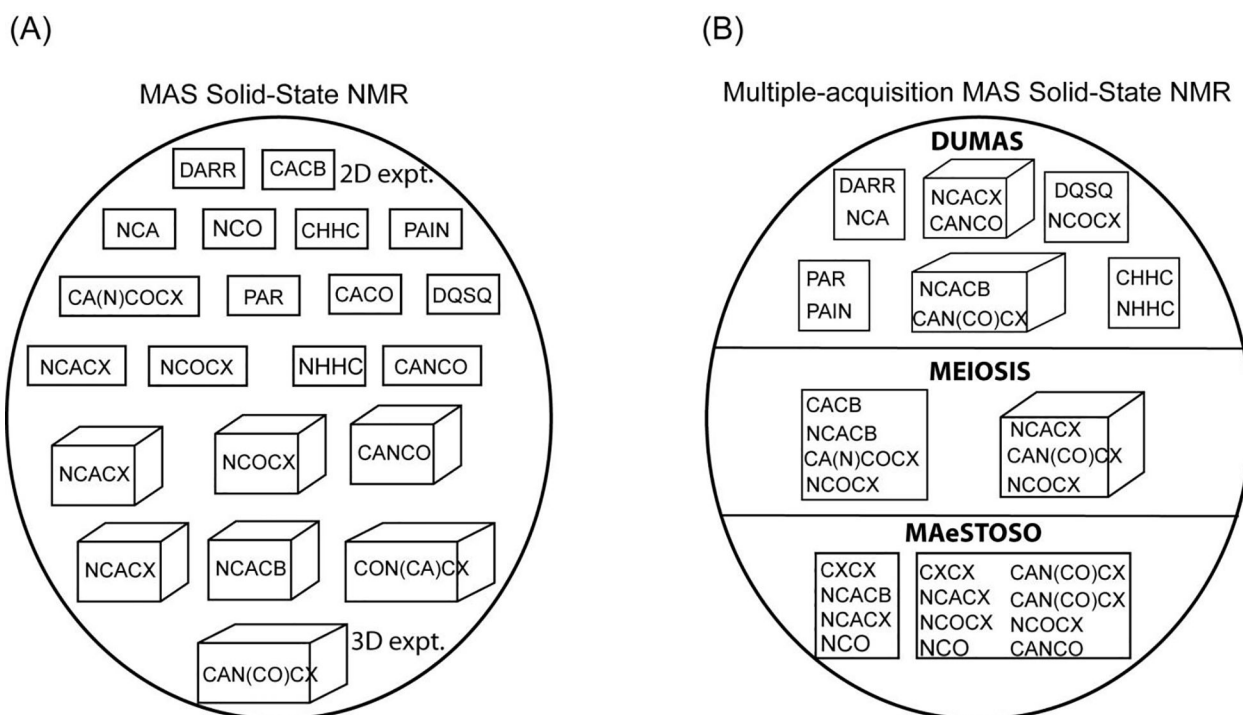
1. Hong M, Zhang Y & Hu F Membrane protein structure and dynamics from NMR spectroscopy. *Annu Rev Phys Chem* 63, 1–24, doi:10.1146/annurev-physchem-032511-143731 (2012). [PubMed: 22136620]
2. McDermott A in Annual Review of Biophysics Vol. 38 Annual Review of Biophysics 385–403 (2009).
3. Siegal G, van Duynhoven J & Baldus M Biomolecular NMR: recent advances in liquids, solids and screening. *Current Opinion in Chemical Biology* 3, 530–536, doi:10.1016/s1367-5931(99)00004-6 (1999). [PubMed: 10508666]
4. Gopinath T, Mote KR & Veglia G Sensitivity and resolution enhancement of oriented solid-state NMR: Application to membrane proteins. *Prog Nucl Magn Reson Spectrosc* 75, 50–68, doi: 10.1016/j.pnmrs.2013.07.004 (2013). [PubMed: 24160761]
5. Baldus M ICMRBS founder's medal 2006: Biological solid-state NMR, methods and applications. *Journal of Biomolecular Nmr* 39, 73–86, doi:10.1007/s10858-007-9177-3 (2007). [PubMed: 17657566]
6. Mainz A et al. The chaperone alphaB-crystallin uses different interfaces to capture an amorphous and an amyloid client. *Nature structural & molecular biology* 22, 898–905, doi:10.1038/nsmb.3108 (2015).
7. Vostrikov VV et al. Ca(2+) ATPase Conformational Transitions in Lipid Bilayers Mapped by Site-directed Ethylation and Solid-State NMR. *ACS chemical biology* 11, 329–334, doi:10.1021/acscchembio.5b00953 (2016). [PubMed: 26650884]

8. Wang S & Ladizhansky V Recent advances in magic angle spinning solid state NMR of membrane proteins. *Prog Nucl Magn Reson Spectrosc* 82C, 1–26, doi:10.1016/j.pnmrs.2014.07.001 (2014).
9. Sharma M et al. Insight into the mechanism of the influenza A proton channel from a structure in a lipid bilayer. *Science* 330, 509–512, doi:10.1126/science.1191750 (2010). [PubMed: 20966252]
10. Gustavsson M et al. Allosteric regulation of SERCA by phosphorylation-mediated conformational shift of phospholamban. *Proc Natl Acad Sci U S A* 110, 17338–17343, doi:10.1073/pnas.1303006110 (2013). [PubMed: 24101520]
11. Hu F, Luo W & Hong M Mechanisms of proton conduction and gating in influenza M2 proton channels from solid-state NMR. *Science* 330, 505–508, doi:10.1126/science.1191714 (2010). [PubMed: 20966251]
12. Lange A et al. Toxin-induced conformational changes in a potassium channel revealed by solid-state NMR. *Nature* 440, 959–962, doi:10.1038/nature04649 (2006). [PubMed: 16612389]
13. Gor'kov PL et al. Using low-E resonators to reduce RF heating in biological samples for static solid-state NMR up to 900 MHz. *Journal of magnetic resonance* 185, 77–93, doi:10.1016/j.jmr.2006.11.008 (2007). [PubMed: 17174130]
14. McNeill SA, Gor'kov PL, Shetty K, Brey WW & Long JR A low-E magic angle spinning probe for biological solid state NMR at 750 MHz. *Journal of magnetic resonance* 197, 135–144, doi:10.1016/j.jmr.2008.12.008 (2009). [PubMed: 19138870]
15. Stringer JA et al. Reduction of RF-induced sample heating with a scroll coil resonator structure for solid-state NMR probes. *Journal of magnetic resonance* 173, 40–48, doi:10.1016/j.jmr.2004.11.015 (2005). [PubMed: 15705511]
16. Maly T et al. Dynamic nuclear polarization at high magnetic fields. *J Chem Phys* 128, 052211, doi:10.1063/1.2833582 (2008). [PubMed: 18266416]
17. Rossini AJ et al. Dynamic nuclear polarization surface enhanced NMR spectroscopy. *Acc Chem Res* 46, 1942–1951, doi:10.1021/ar300322x (2013). [PubMed: 23517009]
18. Wickramasinghe NP et al. Nanomole-scale protein solid-state NMR by breaking intrinsic 1HT1 boundaries. *Nat Methods* 6, 215–218, doi:10.1038/nmeth.1300 (2009). [PubMed: 19198596]
19. Reif B Ultra-high resolution in MAS solid-state NMR of perdeuterated proteins: implications for structure and dynamics. *J Magn Reson* 216, 1–12, doi:10.1016/j.jmr.2011.12.017 (2012). [PubMed: 22280934]
20. Agarwal V et al. De Novo 3D Structure Determination from Sub-milligram Protein Samples by Solid-State 100 kHz MAS NMR Spectroscopy. *Angew Chem Int Ed Engl*, doi:10.1002/anie.201405730 (2014).
21. Gopinath T & Veglia G 3D DUMAS: simultaneous acquisition of three-dimensional magic angle spinning solid-state NMR experiments of proteins. *J Magn Reson* 220, 79–84, doi:10.1016/j.jmr.2012.04.006 (2012). [PubMed: 22698806]
22. Gopinath T & Veglia G Dual acquisition magic-angle spinning solid-state NMR-spectroscopy: simultaneous acquisition of multidimensional spectra of biomacromolecules. *Angew Chem Int Ed Engl* 51, 2731–2735, doi:10.1002/anie.201108132 (2012). [PubMed: 22311700]
23. Gopinath T & Veglia G Orphan spin operators enable the acquisition of multiple 2D and 3D magic angle spinning solid-state NMR spectra. *J Chem Phys* 138, 184201, doi:10.1063/1.4803126 (2013). [PubMed: 23676036]
24. Gopinath T & Veglia G Multiple acquisition of magic angle spinning solid-state NMR experiments using one receiver: application to microcrystalline and membrane protein preparations. *Journal of magnetic resonance* 253, 143–153, doi:10.1016/j.jmr.2015.01.001 (2015). [PubMed: 25797011]
25. Gopinath T & Veglia G Multiple acquisitions via sequential transfer of orphan spin polarization (MAeSTOSO): How far can we push residual spin polarization in solid-state NMR? *Journal of magnetic resonance* 267, 1–8, doi:10.1016/j.jmr.2016.03.001 (2016). [PubMed: 27039168]
26. Mote KR, Gopinath T & Veglia G Determination of structural topology of a membrane protein in lipid bilayers using polarization optimized experiments (POE) for static and MAS solid state NMR spectroscopy. *J Biomol NMR* 57, 91–102, doi:10.1007/s10858-013-9766-2 (2013). [PubMed: 23963722]

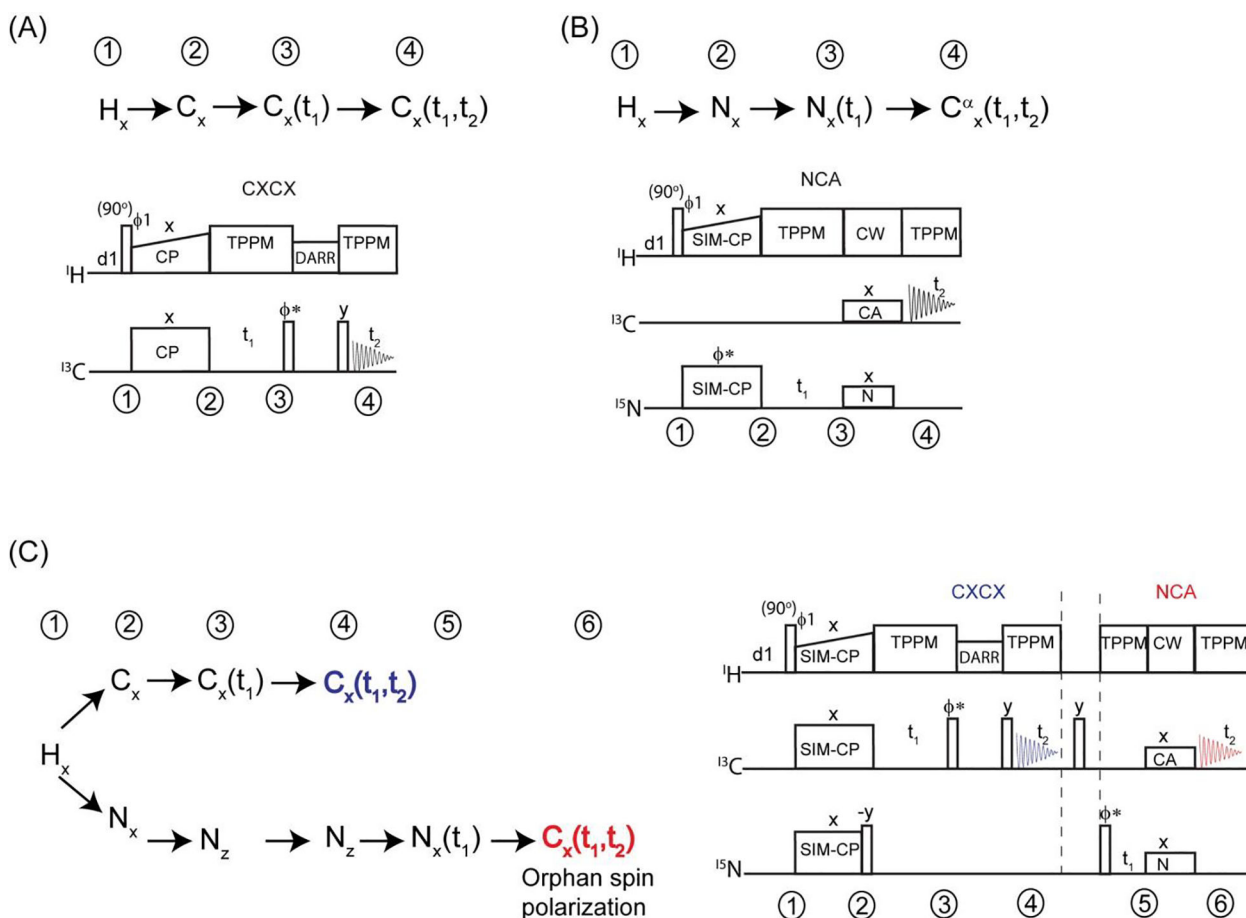
27. Giraud N et al. Site-specific backbone dynamics from a crystalline protein by solid-state NMR spectroscopy. *Journal of the American Chemical Society* 126, 11422–11423, doi:10.1021/ja046578g (2004). [PubMed: 15366872]
28. Chevelkov V, Zhuravleva AV, Xue Y, Reif B & Skrynnikov NR Combined analysis of  $(15)\text{N}$  relaxation data from solid- and solution-state NMR spectroscopy. *Journal of the American Chemical Society* 129, 12594–12595, doi:10.1021/ja073234s (2007). [PubMed: 17902660]
29. Pines A, Gibby MG & Waugh JS Proton-enhanced NMR of dilute spins in solids. *J Chem Phys* 59, 569–590 (1973).
30. Takegoshi K, Nakamura S & Terao T C-13-H-1 dipolar-assisted rotational resonance in magic-angle spinning NMR. *Chemical Physics Letters* 344, 631–637, doi:10.1016/s0009-2614(01)00791-6 (2001).
31. Baldus M, Petkova AT, Herzfeld J & Griffin RG Cross polarization in the tilted frame: assignment and spectral simplification in heteronuclear spin systems. *Molecular Physics* 95, 1197–1207 (1998).
32. Hartmann SR & Hahn EL Nuclear Double Resonance in the Rotating Frame. *Physical Review* 128, 2042–2053 (1962).
33. Griffiths JM et al. ROTATIONAL RESONANCE SOLID-STATE NMR ELUCIDATES A STRUCTURAL MODEL OF PANCREATIC AMYLOID. *Journal of the American Chemical Society* 117, 3539–3546, doi:10.1021/ja00117a023 (1995).
34. Castellani F et al. Structure of a protein determined by solid-state magic-angle-spinning NMR spectroscopy. *Nature* 420, 98–102, doi:10.1038/nature01070 (2002). [PubMed: 12422222]
35. Levitt MH, Suter D & Ernst RR Spin dynamics and thermodynamics in solid-state NMR cross polarization. *The Journal of chemical physics* 84, 4243, doi:10.1063/1.450046 (1986).
36. Ader C et al. Structural rearrangements of membrane proteins probed by water-edited solid-state NMR spectroscopy. *Journal of the American Chemical Society* 131, 170–176, doi:10.1021/ja806306e (2009). [PubMed: 19063626]
37. Banigan JR, Gayen A & Traaseth NJ Combination of  $(1)(5)\text{N}$  reverse labeling and afterglow spectroscopy for assigning membrane protein spectra by magic-angle-spinning solid-state NMR: application to the multidrug resistance protein EmrE. *J Biomol NMR* 55, 391–399, doi:10.1007/s10858-013-9724-z (2013). [PubMed: 23539118]
38. Sinnige T, Daniels M, Baldus M & Weingarth M Proton clouds to measure long-range contacts between nonexchangeable side chain protons in solid-state NMR. *Journal of the American Chemical Society* 136, 4452–4455, doi:10.1021/ja412870m (2014). [PubMed: 24467345]
39. Verardi R, Shi L, Traaseth NJ, Walsh N & Veglia G Structural topology of phospholamban pentamer in lipid bilayers by a hybrid solution and solid-state NMR method. *Proc Natl Acad Sci U S A* 108, 9101–9106, doi:10.1073/pnas.1016535108 (2011). [PubMed: 21576492]
40. Ekanayake EV, Fu R & Cross TA Structural Influences: Cholesterol, Drug, and Proton Binding to Full-Length Influenza A M2 Protein. *Biophysical journal* 110, 1391–1399, doi:10.1016/j.bpj.2015.11.3529 (2016). [PubMed: 27028648]
41. Gurevich AZ, Barsukov IL, Arseniev AS & Bystrov VF Combined COSY-NOESY Experiment. *J Magn Reson* 56, 471–478 (1984).
42. Fukuchi M, Inukai M, Takeda K & Takegoshi K Double-acquisition: Utilization of discarded coherences in a 2D separation experiment using the States method. *Journal of Magnetic Resonance* 194, 300–302, doi:10.1016/j.jmr.2008.07.004 (2008). [PubMed: 18667347]
43. Fukuchi M & Takegoshi K Combination of  $(13)\text{C}$ - $(13)\text{C}$  COSY and DARR (COCODARR) in solid-state NMR. *Solid State Nucl Magn Reson* 34, 151–153, doi:10.1016/j.ssnmr.2008.05.001 (2008). [PubMed: 18635343]
44. Kupce E, Kay LE & Freeman R Detecting the “afterglow” of  $13\text{C}$  NMR in proteins using multiple receivers. *Journal of the American Chemical Society* 132, 18008–18011, doi:10.1021/ja1080025 (2010). [PubMed: 21126087]
45. Banigan JR & Traaseth NJ Utilizing afterglow magnetization from cross-polarization magic-angle-spinning solid-state NMR spectroscopy to obtain simultaneous heteronuclear multidimensional spectra. *J Phys Chem B* 116, 7138–7144, doi:10.1021/jp303269m (2012). [PubMed: 22582831]



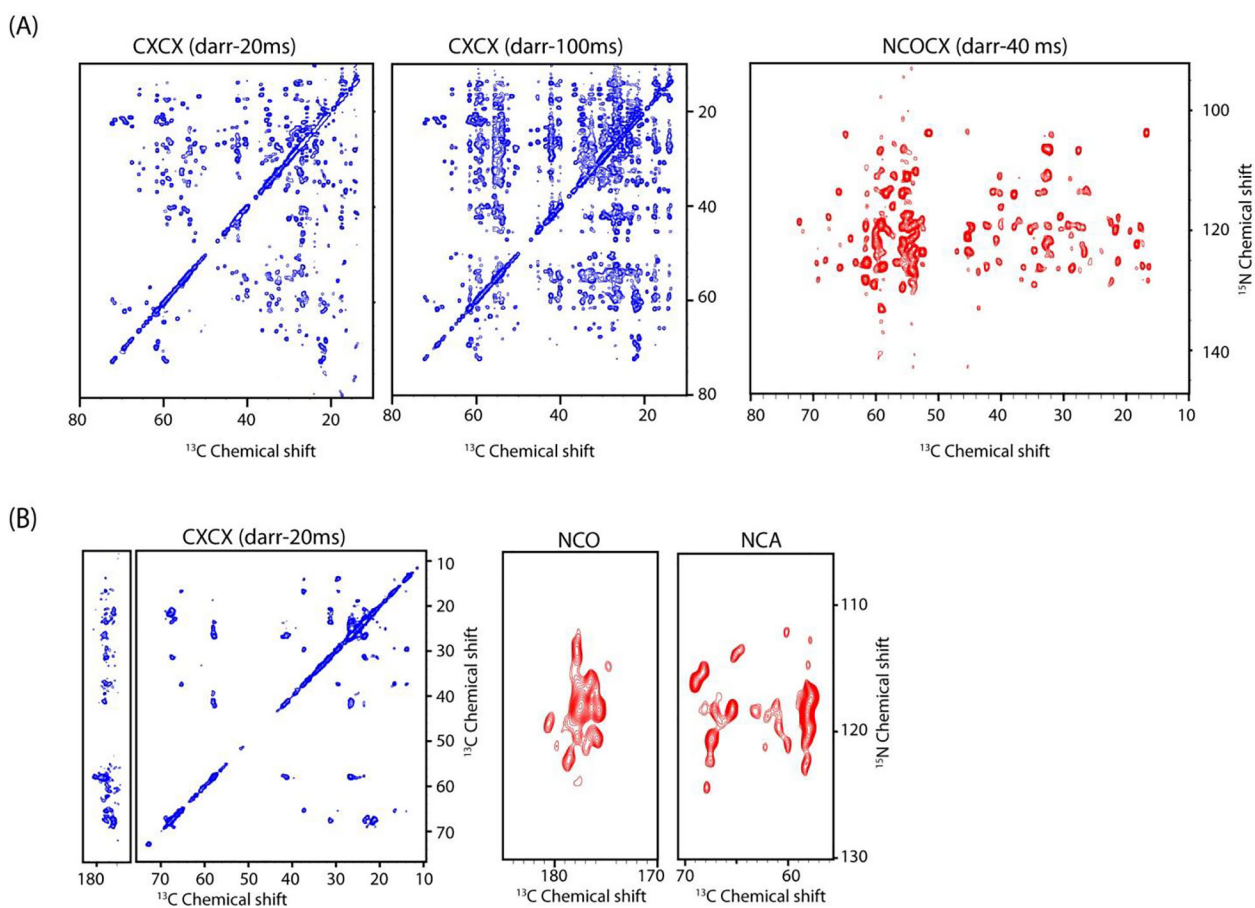
**Figure 1:** Schematic of pulse sequence events for (A) conventional and (B) multiple acquisition 2D MAS ssNMR using single receiver. In the multiple-acquisition approach two to eight 2D experiments are simultaneously acquired in a single experiment.



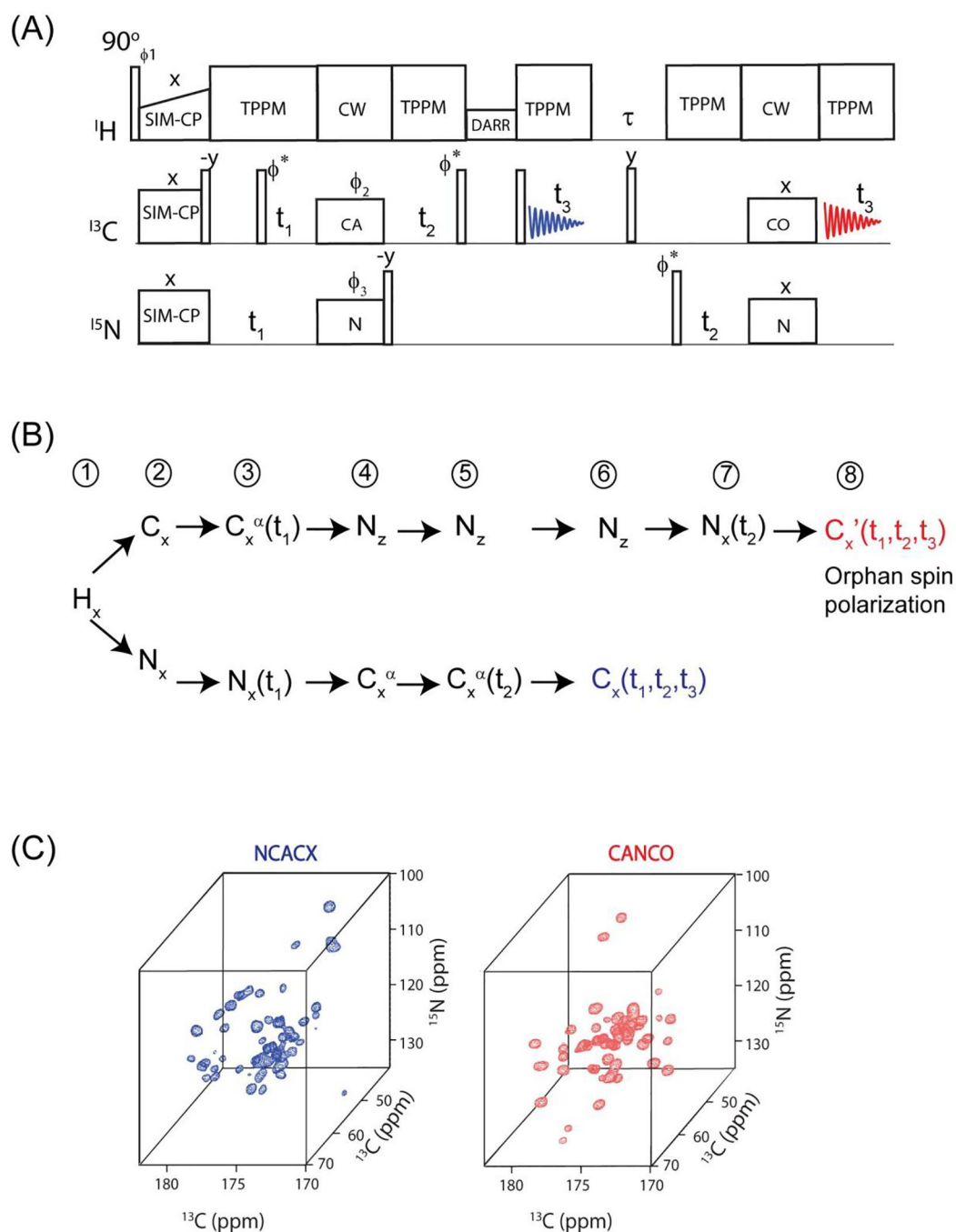
**Figure 2:**  
 (A) Various 2D (represented in square) and 3D (represented in cube) experiments that are used for protein ssNMR. (B) Few examples of DUMAS, MEIOSIS, and MAeSTOSO approaches that combine multiple experiments into a single 2D or 3D experiment represented in rectangle and cube respectively.



**Figure 3:** Pulse sequences and corresponding polarization pathways for conventional (A) CXCX and (B) NCA experiments. (C) Dual polarization pathways that are used for simultaneous acquisition of CXCX and NCA using DUMAS ssNMR.

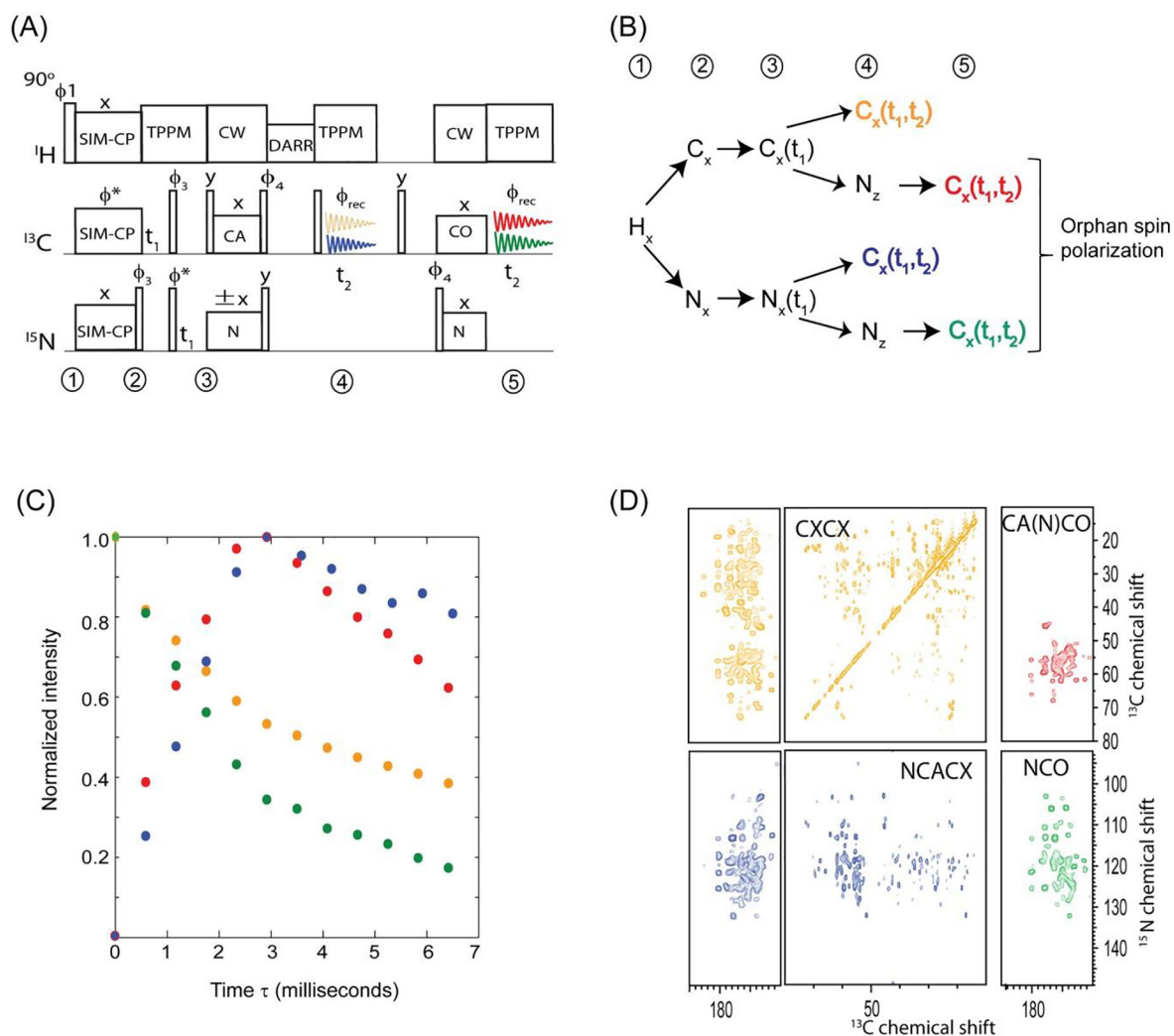


**Figure 4:**  
CXCX and NC correlation spectra of (A) ubiquitin and (B) sarcolipin membrane protein obtained from 2D DUMAS experiments.

**Figure 5:**

(A) An example of 3D DUMAS pulse sequence for simultaneous acquisition of NCACX and CANCO, (B) Evolution of two polarization pathways are acquired in first and second acquisitions. (C) NCACX and CANCO 3D spectra of ubiquitin obtained from the above pulse sequence.



**Figure 6:**

(A) Two-dimensional MEIOSIS pulse sequence for simultaneous acquisition of CXCX, NCACX, CA(N)CO and NCO experiments. (B) Evolution of spin operators during the pulse sequence. (C) Amplitudes of four pathways that are respectively color coded, residual pathways are represented in orange and green colors. (D) MEIOSIS spectra of ubiquitin obtained simultaneously using the pulse sequence shown in (A).

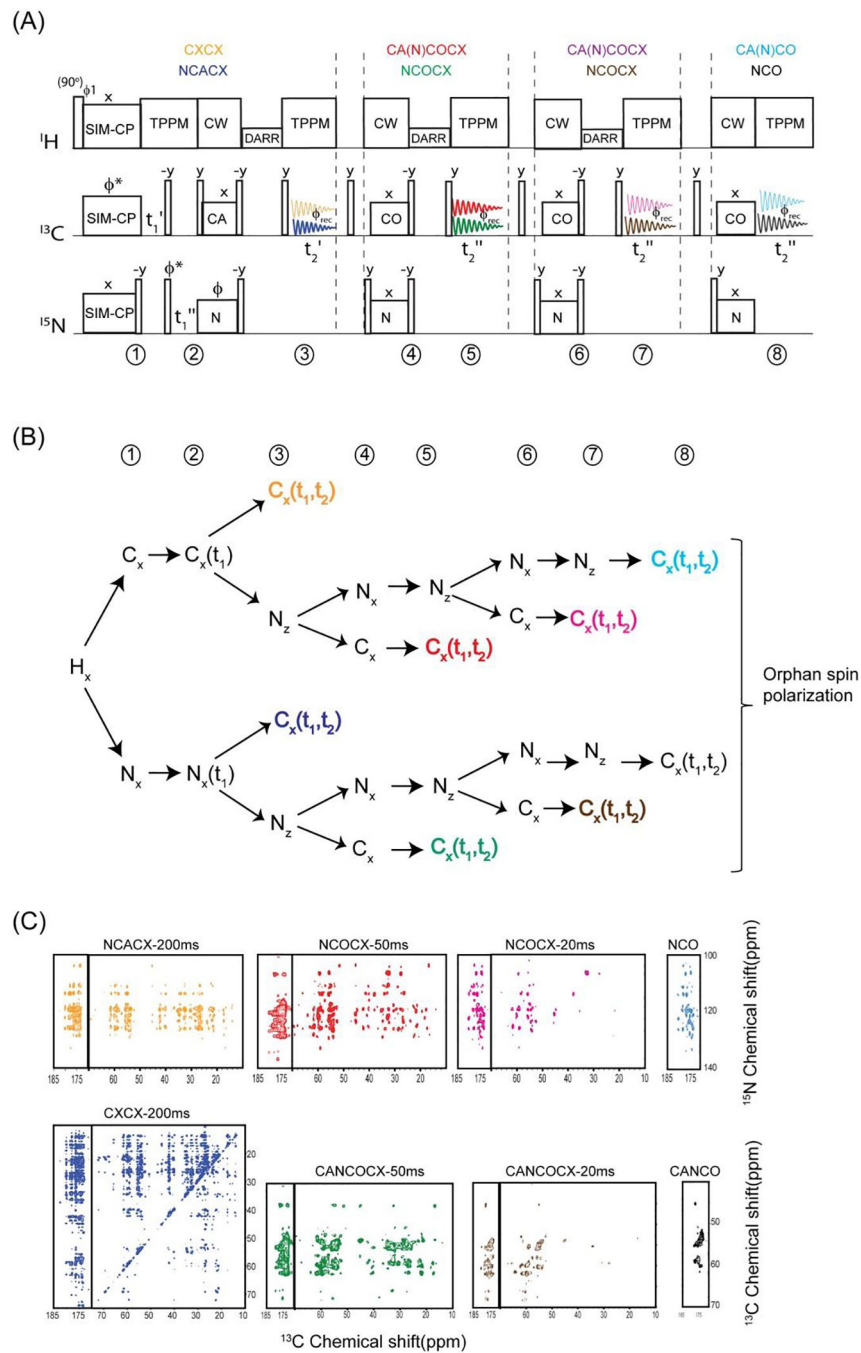


**Figure 7:**  
 (A) MAeSTOSO-8 pulse sequence for simultaneous acquisition on eight 2D experiments.  
 (B) Evolution of spin operators during the course of the pulse sequence. (C) Simultaneous acquisition of eight 2D spectra of  $U^{13}C-^{15}N$  ubiquitin.